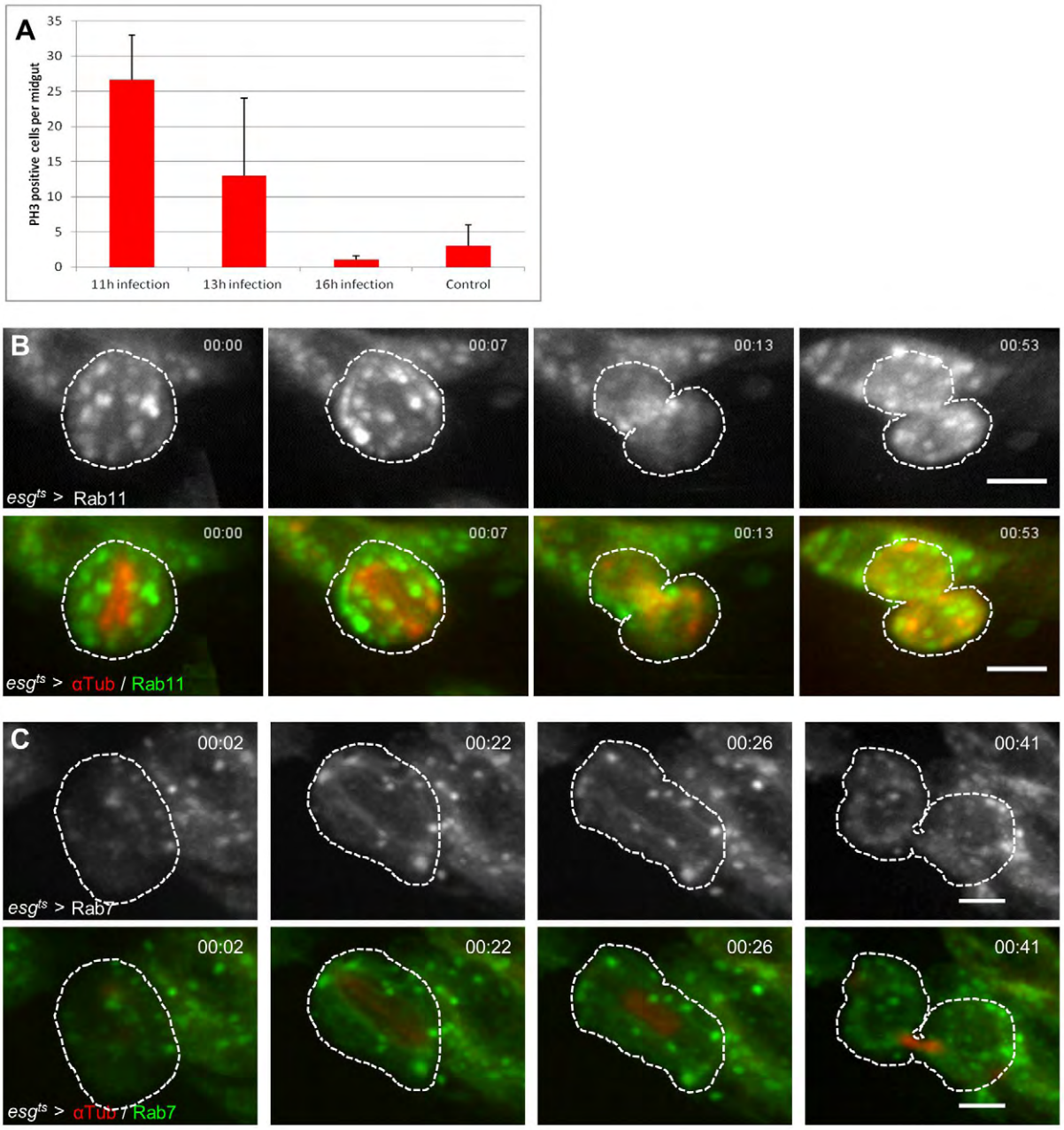

Fig. S1. Proliferation rate depending on infection conditions and random dispatch of recycling and late endosomes during ISC mitosis.

(**A**) Quantification of PH3-positive cells per midgut depending on infection time. Flies orally infected by *Ecc15* during 11 hours exhibit the highest number of dividing ISCs. (11 hours infection N=3 guts, 13 hours infection N=2, 16 hours infection N=3, control N=2) (**B**) Z-projection frames from a movie showing the symmetric segregation of recycling endosomes during ISC mitosis. *UAS-Rab11-GFP* (green in merge) and *UAS-mCherry-αTubulin* (red in merge) are activated under the control of the esg^{ts} system (n=3 cells). Scale bar, 5µm. (**C**) Z-projection frames from a movie showing the random partitioning of late endosomes during ISC mitosis. The *esg-Gal4* driver combined with $tub\text{-}Gal80^{ts}$ was used to express *UAS-Rab7-GFP* (green in merge) and *UAS-mCherry-αTubulin* (red in merge) (n=6 cells) (See Movie 3 in supplementary material). The partitioning of late endosomes is much less asymmetric (on average 65.7%±2.1%, n=6 cells) than Sara endosomes ($p<0.1$; Student t test). Scale bar, 3µm. Dashed line, cell outline.

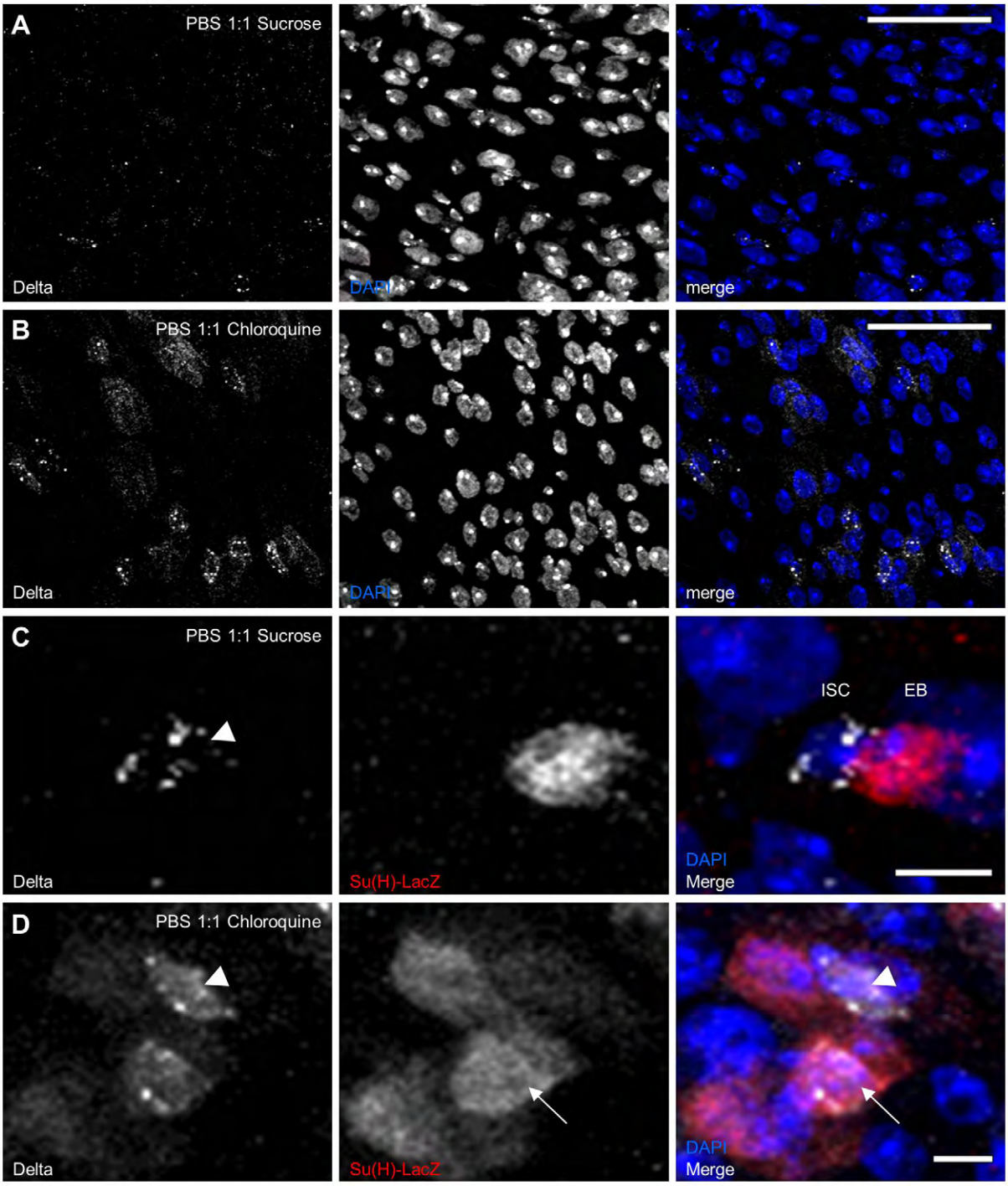

Fig. S2. Lysosomal degration of Delta in EBs.

(**A-D**) Z-projection confocal images of 15 day-old posterior adult midguts labelled with DAPI (blue in merge). ISCs and EBs are identified by Delta (white) and βgalactosidase (red) immunostainings, respectively. (control N=9 guts, chloroquine treatment N=8 guts) (A-B) Blocking lysosomal degradation by chloroquine ingestion during 2 days induces an increase of Delta-positive cells and Delta expression. Scale bars, 30µm. (C-D) Chloroquine treatment delays degradation of Delta. As a consequence Delta is not only seen in ISC (arrowhead) but also in some EBs (arrow), probably representing EBs shortly after mitosis. Scale bars, 5µm.

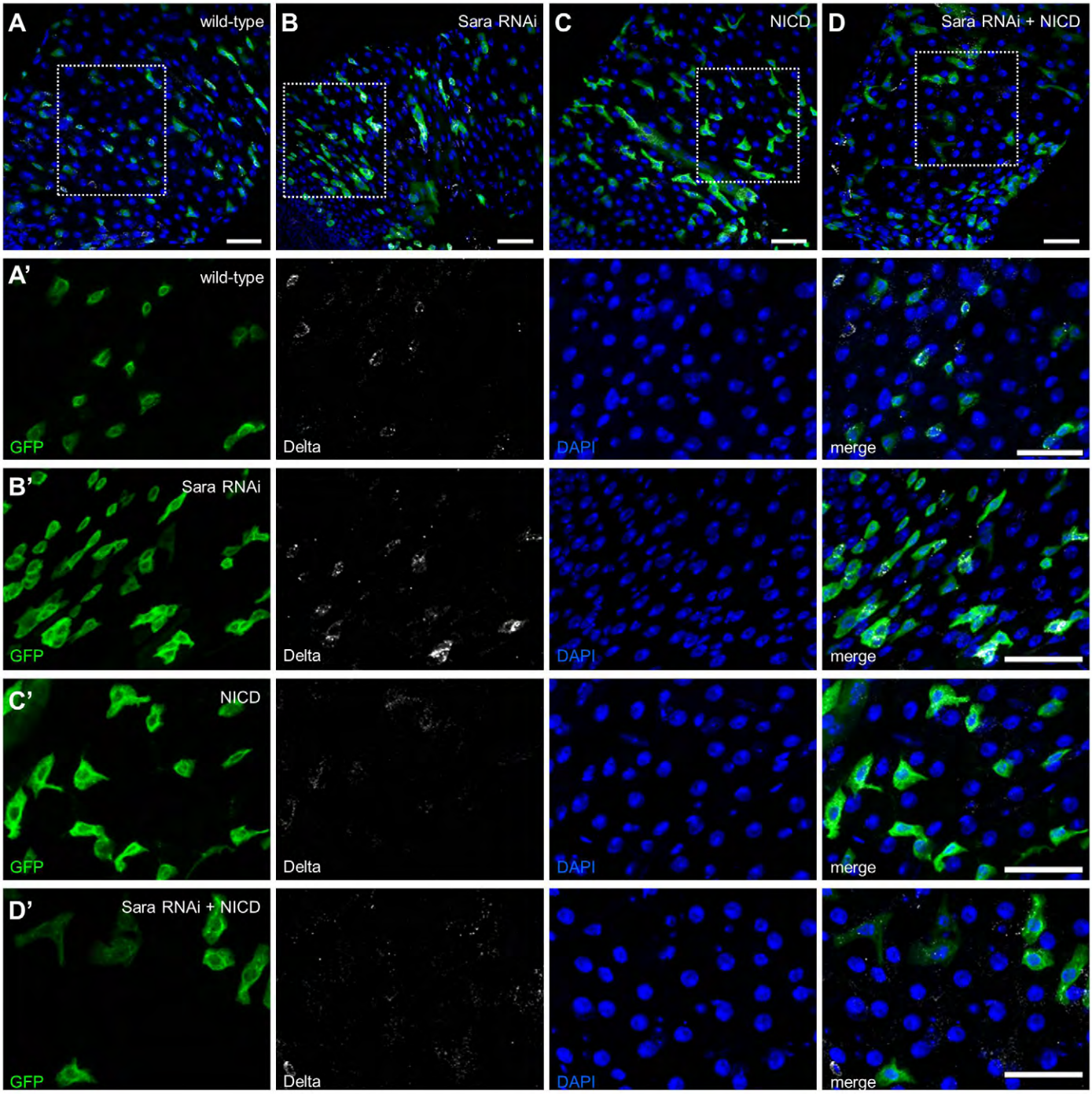

Fig. S3. Notch signalling is downstream of Sara.

(**A-D**) Effect of Sara and Notch in *esg*-positive cells using *UAS-Sara-RNAi* and/or *UAS-Notch*^{cdc10} transgenes. Z-projection confocal images of GFP-positively marked cells expressing different contructs. Dashed boxes in A-D mark the regions showed as rotated close-ups in A'-D'. (A-A',B-B') Sara RNAi (N=20 guts) leads to an accumulation of Delta-positive cells compared to wild-type (N=14guts), similar to *Sara*^{12} mutant phenotype. (C-C',D-D') The constitutive activation of the intracellular domain of Notch (NICD, N=15 guts) and the genetic interaction with Sara RNAi (N=15 guts) show similar increase of cells with large nuclei corresponding to ECs. This indicates that Notch signalling acts downstream of Sara function. Scale bars, 30μm. For genotypes, see materials and methods.

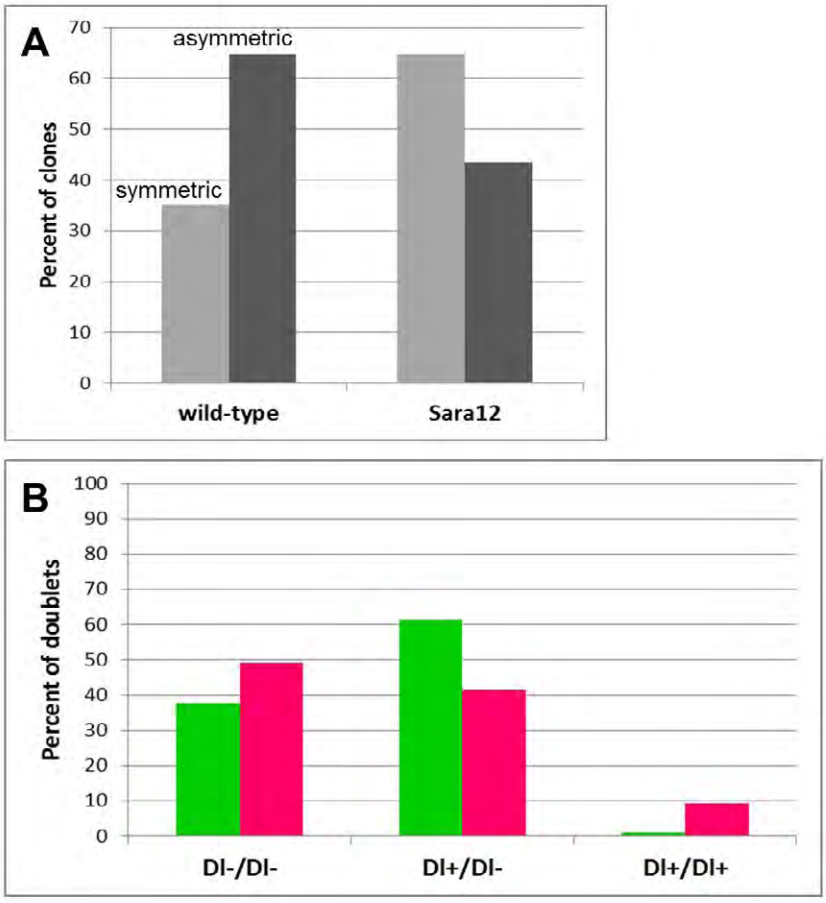

Fig. S4. Preponderant asymmetric division of ISCs in adult *Drosophila* midguts.
(**A**) Quantification of symmetric versus asymmetric ISC division in 15 day-old adult midguts. The frequency of asymmetric divisions are defined by the presence of a single Delta-positive cell per clone, relative to the total number of multiple cell clones (wild-type n=171 clones, $Sara^{12}$ n=85). The absence of Sara leads to an increase in symmetric ISC division. (**B**) Proportion of Delta-positive cells in doublets (wild-type n=101 doublets, $Sara^{12}$ n=53).

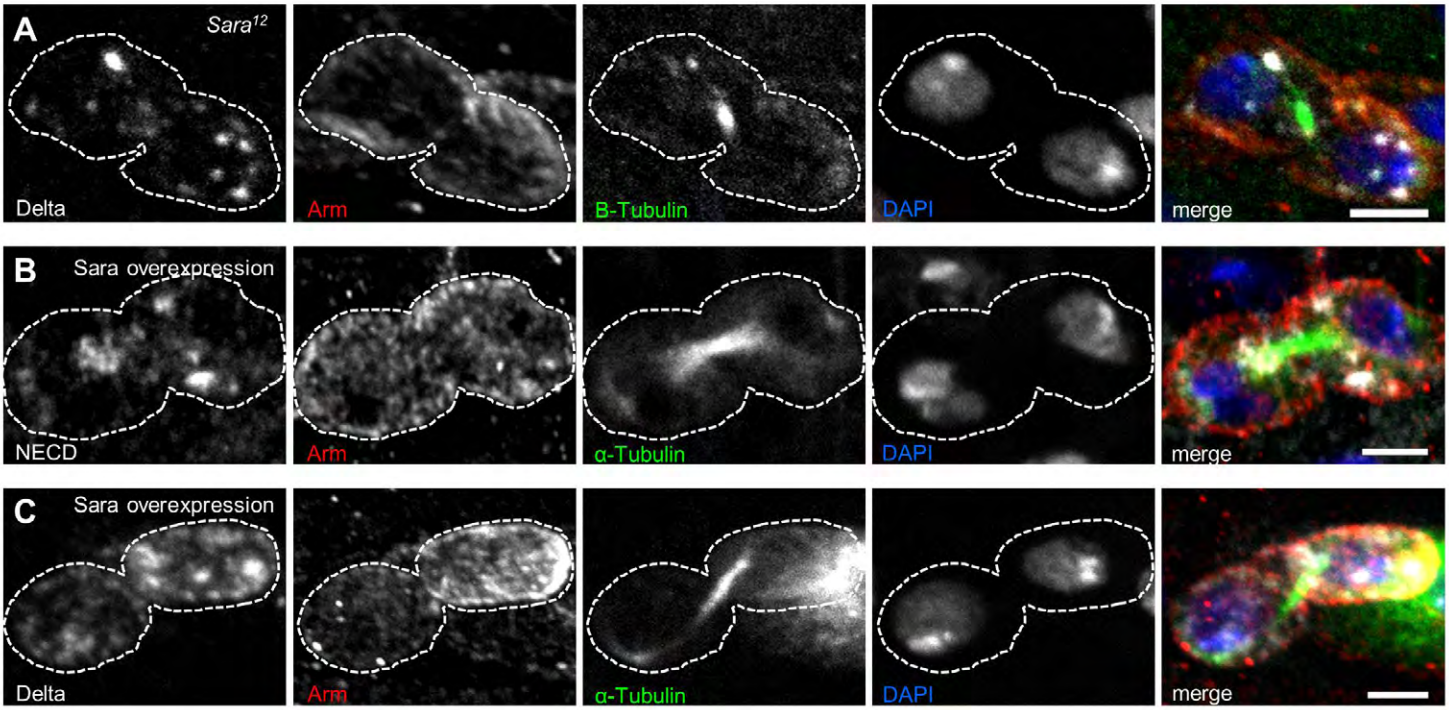

Fig. S5. Symmetric ISC division in Sara loss of function and Sara overexpression.
(**A-C**) Z-projection confocal images of dividing ISCs at cytokinesis. The cell border and nuclei are labelled by Armadillo (Arm, red in merge) and DAPI (blue) immunostainings, respectively. (A) The mitotic spindle is visualized by E7-488 immunostaining. In absence of Sara, Delta (white) segregates symmetrically during mitosis (54.64% versus 45.36% in the two future daughter cells). (B-C) *UAS-mCherry-αTubulin* (green in merge) expressed under the control of *esg-Gal4* driver combined with *tug-Gal80^{ts}* and detected by a ds-red immunostaining. In Sara overexpressing ISCs, Notch (52.56% versus 47.44% in these cells) and Delta (67.37% versus 32.64%, n=7 cells) are symmetrically partitioned at cytokinesis. Dashed line, cell outlines. Scale bars, 3µm.

Movie 1. Directional partitioning of Sara endosomes upon *Ecc15* infection.
Sara endosomes (green) and the mitotic spindle (α-Tubulin-GFP, red) are observed 11 hours after *Ecc15* oral infection. Scale bar, 5 µm.

Movie 2. Asymmetric segregation of Sara endosomes during ISC mitosis.
The behaviour of Sara endosomes (green) and the mitotic spindle (mCherry-βTubulin, red) is observed during ISC division (no infection). Scale bar, 5 μm.

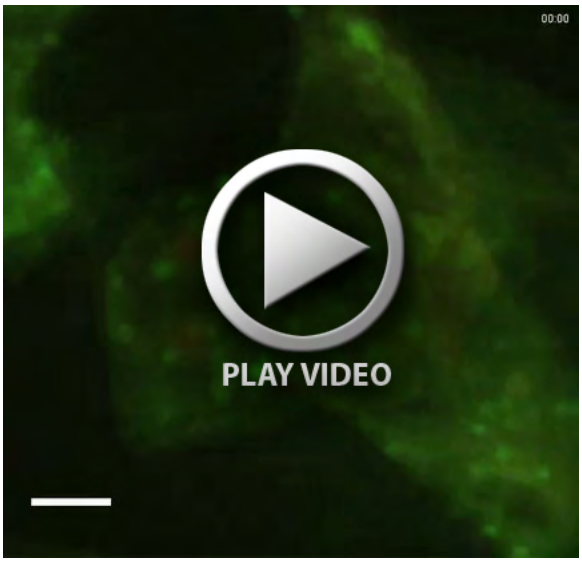

Movie 3. Random partitioning of late endosomes during ISC mitosis.
Late endosomes labelled with Rab7-GFP (green) and the mitotic spindle (mCherry-α-Tubulin, red) are observed during ISC division. Scale bar, 3 μm.

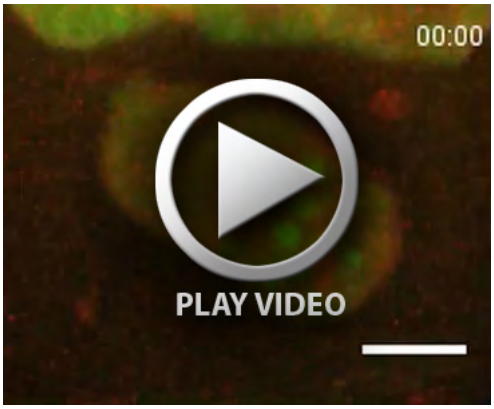

Movie 4. Asymmetric dispatch of the Pon cortical factor during ISC mitosis.
Pon^{LD}-RFP (red) forms a crescent perpendicularly aligned with the mitotic spindle (lines in red in the middle of the dividing ISC). At the end of mitosis, Pon crescent is asymmetrically inherited by the ISC daughter cell. Sara endosomes are delivered in the Pon-negative cell, which corresponds to the presumptive EB. Scale bar, 5 μm.